Sobolev scalar products in the construction of velocity models

*Petr Bulant and Luděk Klimeš *, Charles University, Prague, Czech Republic*
E-mails: bulant@seis.karlov.mff.cuni.cz, klimes@seis.karlov.mff.cuni.cz

Summary

The minimization of the Sobolev norm during linearized inversion of given data enables to control the model parameters unresolved by the data being fitted.

Even if a reasonably looking model can be obtained without minimizing the Sobolev norm, it may be too rough for some computational methods. We may construct models optimally smooth for given computational methods by minimizing the corresponding Sobolev norm during the inversion.

Probably the smoothest models are required by the ray methods. The efficiency of ray tracing can be evaluated in terms of the "average Lyapunov exponent" for the model. The "average Lyapunov exponent" may be approximated by the square root of the corresponding Sobolev norm of the model, which allows models optimum for ray tracing to be constructed.

1 Sobolev scalar products and Sobolev norms

We define the Sobolev scalar product (see, e.g., Tarantola 1987) of real–valued functions f and g as a linear combination of the L_2 Lebesgue scalar products of the zero, first, second or higher derivatives of the functions:

$$((f,g)) = \left[\int \mathrm{dx}\right]^{-1} \sum_{ij\ldots} \sum_{ab\ldots} \int \mathrm{dx}\; b_{ij\ldots|ab\ldots}\; f_{,ij\ldots}(x_p)\; g_{,ab\ldots}(x_q) \quad , \tag{1}$$

where $\int \mathrm{dx}$ is the definite integral over the model volume, and $b_{ij\ldots|ab\ldots}$ are real-valued coefficients of the linear combination. The linear combination should preserve the properties required of scalar products (symmetry and positiveness). The maximum number of indices $ij\ldots$ and $ab\ldots$ in (1) equals the maximum order of the considered derivatives, the indices take the values from 1 to 3 in 3-D, 1 to 2 in 2-D and 1 in 1-D.

The Sobolev norm of a velocity model may, in general, be composed of the zero, first, second or higher derivatives of the functions describing the model. The model is very often described by cubic, bicubic or tricubic splines. Since the third homogeneous partial derivatives of the splines are discontinuous, the Sobolev scalar product composed of the fourth and higher derivatives could be infinite, and thus should be avoided. Simultaneously, minimization of the (zero derivatives of the) model functions usually has no meaning. We thus usually consider only Sobolev norms composed of the first, second and third derivatives. Since studies of the third derivatives have not yet been finished, we will concentrate on the first and second derivatives.

2 Including the Sobolev norm in the objective function for inversion of seismic data

The minimization of the Sobolev norm during linearized inversion of given data enables to control the model parameters unresolved by the data being fitted. For example, if we are fitting discrete values of a material parameter with a smooth function, the properties of interpolation between the discrete values may be controlled by means of minimizing the square of the selected Sobolev norm of the function.

Even if a reasonably looking model can be obtained without minimizing the Sobolev norm, it may be too rough for some computational methods. The errors of many computational methods may be approximated by a function dependent on the Sobolev norm of functions describing the model. We may thus construct models optimally smooth for given computational methods.

In the case of ray methods, the situation is more complicated. The feasibility and efficiency of ray tracing imposes relatively strong requirements on the smoothness of the velocity models, but, unfortunately, we still have no quantitative criteria of applicability and accuracy of ray methods or their extensions. On the other hand, the numerical efficiency of ray tracing can be evaluated in terms of the "average Lyapunov exponent", introduced by Klimeš (2002a) for 2-D models without structural interfaces.

Sobolev norms in model building

2.1 Fitting discrete values and regularizing an ill–conditioned inversion

Assume that we are fitting discrete values u^α at points $\mathbf{x}^\alpha$ inside the model volume by minimizing objective function

$$y = \sum_\alpha [\tilde{u}(\mathbf{x}^\alpha) - u^\alpha]^2 [\Delta u^\alpha]^{-2} + S^2((\tilde{u}, \tilde{u})) \quad , \tag{2}$$

where Δu^α is a given standard deviation of model $\tilde{u}(\mathbf{x})$ from values u^α at points $\mathbf{x} = \mathbf{x}^\alpha$. For infinitely small weighting factor $S \to 0$, the limit form $\tilde{\tilde{u}}(\mathbf{x}) = \lim_{S \to 0} \tilde{u}(\mathbf{x})$ of the solution corresponds to the minimization of objective function $y = ((\tilde{u}, \tilde{u}))$ with boundary conditions $\tilde{\tilde{u}}(\mathbf{x}^\alpha) = u^\alpha$.

The properties of interpolation between discrete values by means of minimizing the squares of different Sobolev norms has been investigated by Klimeš (2000). He showed that the Sobolev norm composed of second derivatives of model functions is suitable for fitting discrete values.

Assume that we are fitting a structural interface with a smooth function. In such a case the data for the function are available only in that part of the model, where the interface is located. The behaviour of the function in other parts of the model is not given by the data, see Figure 3. We might control the function by adding new artificial points to the data for the interface, but this manual intervention would probably slightly distort the modelled interface. It is much more convenient to control the function by increasing the weighting factor S of the Sobolev norm. A small increment of S will not influence the function in the region with the data, but will regularize its behaviour in the remaining parts of the model.

2.2 Constructing seismic models of optimal smoothness for a selected numerical method

The Sobolev norm is usually included in the inversion of seismic data if the numerical method to be applied to the model requires a smooth model. The Sobolev norm included in the objective function acts as a low–pass wavenumber filter (Klimeš 2000).

We assume the objective function for the inversion of slowness or velocity $u(\mathbf{x})$ in the form of

$$y = \left[\int \mathrm{d}\mathbf{x}\right]^{-1} \int \mathrm{d}\mathbf{x}\, \tilde{C}(\mathbf{x}, \mathbf{x}) + S^2 \|u\|^2 \quad , \tag{3}$$

where $\tilde{C}(\mathbf{x}, \mathbf{x})$ is the covariance function describing the deviation of model $\tilde{u}(\mathbf{x})$ from geological structure $u(\mathbf{x})$ (Klimeš 2002b), and S is the weighting factor of the Sobolev norm $\|u\|$ of the functions describing the model.

The first summand in (3) is the mean squared difference between the model and the geological structure. It is then advantageous if $S\|u\|$ approximates the r.m.s. difference of the results of the numerical method under consideration from the exact solution in the model, expressed in the units of $u(\mathbf{x})$. Objective function (3) then gains the clear physical meaning of the squared deviation between the model and the geological structure plus the squared deviation between the exact and the numerical results in the model, expressed in the units of $u(\mathbf{x})$.

The selection of the Sobolev scalar products for particular numerical methods has been demonstrated by Klimeš (2000) on examples of centred finite differences of the second order, network shortest–path ray tracing, 2-D first–order grid travel time tracing, and 2-D second–order grid travel time tracing.

2.3 Constructing seismic models for ray tracing and Kirchhoff migrations

In complex models, the behaviour of rays becomes chaotic and the geometrical spreading, number of arrivals and density of caustic surfaces increase exponentially with travel time. The exponential increment may be quantitatively described in terms of the "average Lyapunov exponent" for the model. The "average Lyapunov exponent" may roughly be approximated by the square root of the Sobolev norm composed of the second partial derivatives of the functions describing the slowness or velocity field in the model (Klimeš 2000). This enables us to determine the quantitative criteria on models, so as to be suitable for ray tracing, in terms of Sobolev scalar products. We choose the maximum "average Lyapunov exponent" for the model, we estimate the maximum Sobolev norm of the model, and we estimate the value of weighting factor S. We then perform the inversion, compute the values of the "average Lyapunov exponent" and the Sobolev norm in the inverted model, re-estimate the value of S, and continue iteratively with the inversion until we obtain the model of the required smoothness.

3 Numerical examples

Routines for application of the above described minimization of the Sobolev norm during the seismic inversion have been coded in Fortran 77. All the computations are carried out on a PC Pentium with 64 Mbytes of memory. The software used for the computations is available at http://sw3d.mff.cuni.cz .

3.1 Smoothing 2-D model Hess for Kirchhoff migrations

The 2-D model Hess has horizontal dimension 40200 feet and vertical dimension 21000 feet. Two interfaces in the model, limiting a salt body, are discretized on a grid of 64 points spaced at 200 feet. Background velocities are discretized on a grid of 202×106 points with a spacing of $200\,\mathrm{ft} \times 200\,\mathrm{ft}$; the velocity inside the salt body is constant. Originally, each data point is considered to be a model spline point, and the number of model parameters is thus $64 + 64 + 1 + 202 \times 106 = 21541$. See Figure 1.

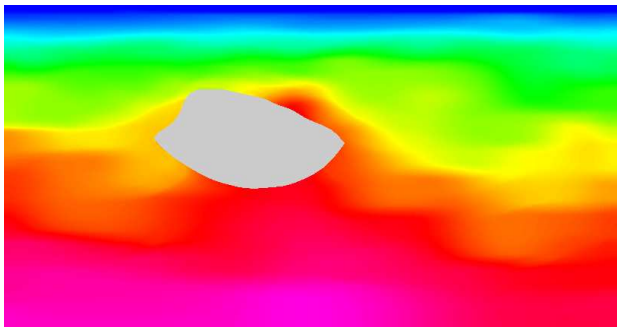

Figure 1: P-wave velocity in the original model Hess. Horizontal dimension of the model is 40200 feet, its vertical dimension is 21000 feet. The background velocity varies from $5000\,\mathrm{ft\,s^{-1}}$ at the top of the model to $9800\,\mathrm{ft\,s^{-1}}$ at the bottom. The velocity of the salt body is constant and equals $14800\,\mathrm{ft\,s^{-1}}$.

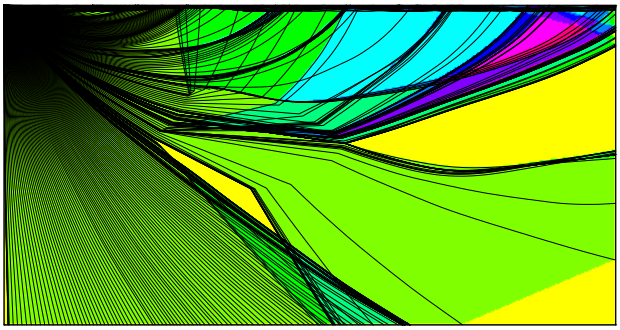

Figure 2: The numbers of travel times and the rays computed for the refracted wave in the original model Hess. The point source is located in the top left corner of the model. The yellow colour corresponds to no travel time, green to 2 arrivals, cyan to 4, blue to 6, magenta to 8, red to 10 arrivals. The maximum number of arrivals is 11.

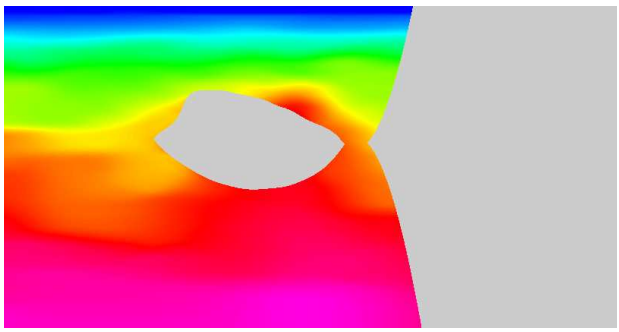

Figure 3: Inversion of the interfaces without the Sobolev norm in the model Hess. The oscillations of the surfaces limiting the lenticular salt body produced another spurious salt body on the right–hand side of the model.

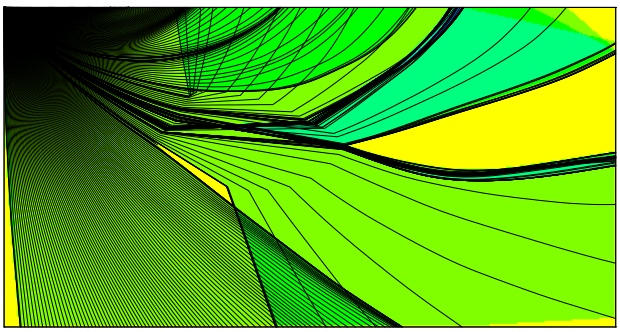

Figure 4: The numbers of travel times and the rays computed for the refracted wave in the smoothed model Hess. The source is again located in the left top corner of the model, the colour scale is the same as in Fig. 2. The maximum number of arrivals is 5.

We perform several tests of ray tracing in the original model. The behaviour of the ray field seems to be too complicated with too many caustics, especially in the low velocity channel near the surface of the model, see Figure 2. We thus decide to smooth the model by means of inversion of the given data with minimization of the Sobolev norms of the velocity field in the model.

We choose a new parameterization of the model as follows: For the interfaces we take an irregular B–spline grid of 28 points with 26 points regularly spaced at 500 feet in the region of the salt body and 2 points at the sides of the model. The two points enable us to control the behaviour of the functions describing the interfaces in the parts of

model not covered by the data for the interfaces, see Figure 3. For the background velocity, we take a horizontally regular grid of 26 points spaced at 1600 feet and a vertically irregular grid of 58 points spaced at 200 feet at the top to 400 feet at the bottom. The number of model parameters is thus $28 + 28 + 1 + 26 \times 58 = 1565$.

The standard relative velocity deviation of the velocity in the inverted model from the velocity in the original model is 0.18 %. The standard deviation of the interfaces is 5.6 ft, which causes a travel time error of approximately $3.15\ 10^{-4}$ s. Figure 4 shows, how the smoothing of the velocity field by including the Sobolev norm in the velocity inversion regularizes the chaotic behaviour of rays.

3.2 Smoothing 2-D model Pluto 1.5

The grided velocities for 2-D model Pluto 1.5 (Figure 5) were created by Smaart Joint Venture, see http://www.smaartjv.com. The model has horizontal dimension 173975 feet and vertical dimension 30000 feet. The velocities are discretized on a grid of 6960×1201 points with a spacing of 25 ft $\times$ 25 ft. The model contains three salt bodies with constant velocity.

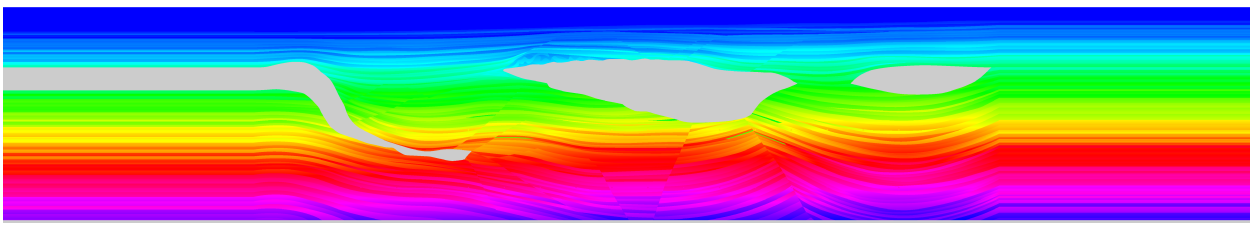

Figure 5: P-wave velocity in the original data grid of 6960 x 1201 points with a spacing of 25 ft x 25 ft in model Pluto 1.5. The background velocity varies from 4920 ft s^{-1} at the top of the model to 13580 ft s^{-1} at the bottom. The velocity of the salt bodies is constant and equals 14800 ft s^{-1}. The horizontal dimension of the model is 173975 ft, its vertical dimension is 30000 ft.

We decided to create a model containing the three salt bodies separated by structural interfaces from the continuous background. We obtain the data for the interfaces from the grided velocities by searching for two neighboring gridpoints, one of them displaying the velocity of the background, and the second one the velocity of the salt. The point of the interface is then taken between such two gridpoints. We cannot use all the identified points at interfaces and all the gridpoints of the velocity grid as the data for inversion due to the limited memory of our computer. We thus use 1009 points at interfaces and a coarser velocity grid of 50×87 points with a spacing of 600 ft $\times$ 2000 ft, and we build the model by means of inversion of the given data with minimization of the Sobolev norms of the velocity field in the model (Figure 6). We choose the parameterization of the model as follows: for the interfaces we take B–spline grid with spline points spaced at 500 feet in the region of the salt body and 2 points at the sides of the model. For the background velocity, we take a regular grid of 38×60 points with a spacing of 800 ft $\times$ 3000 ft.

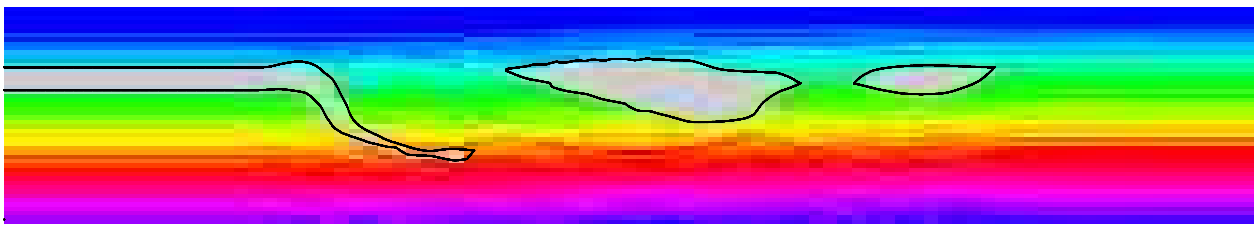

Figure 6: P-wave velocity in the data grid of 50 x 87 points with a spacing of 600 ft x 2000 ft in model Pluto 1.5, plotted together with the points at interfaces identified with the grid spacing of 75 ft. The gridded velocity and the points at interfaces are used as the data for the inversion described in Chapter 3.2. The points at interfaces are plotted by black dots appearing as lines.

The inversion without minimization of the Sobolev norm is ill–conditioned. The inversion with very small weighting factor $S = 1\,000$ ft s of the Sobolev norm yields the velocity model which differs from the given velocities by 3.26 %. The "average Lyapunov exponent" of the model is 0.497 s^{-1}, and the behavior of the rays in the model is too chaotic, see Figure 7. When we perform the inversion with the weighting factor $S = 1\,000\,000$ ft s, we obtain very smooth model with the standard relative velocity deviation 2.71 % and the "average Lyapunov exponent" 0.075 s^{-1}. Figure 9

shows, how the smoothing of the velocity field by including the Sobolev norm in the velocity inversion regularizes the chaotic behaviour of rays. The model with the lowest standard relative velocity deviation has been obtained for the weighting factor $S = 125\,000\,\mathrm{ft\,s}$, see Figure 8. The increment of the standard relative velocity deviation when decreasing the weighting factor from $S = 125\,000\,\mathrm{ft\,s}$ towards $S = 1\,000\,\mathrm{ft\,s}$ indicates an ill-conditioned inversion.

Note that in this example the velocity deviation is caused rather by insufficient B-spline sampling then by smoothing.

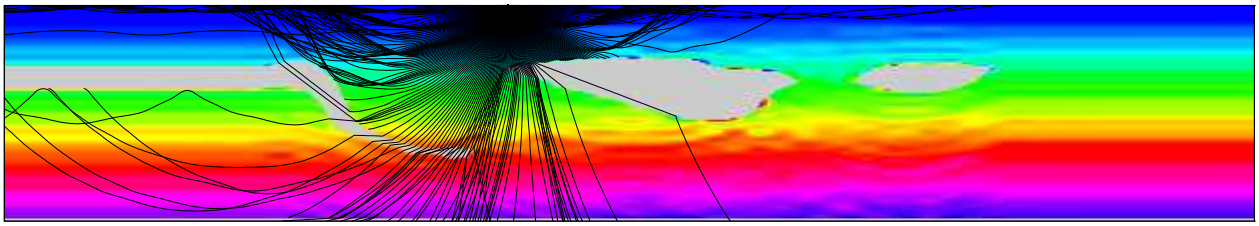

Figure 7: Rays computed by one–parametric shooting in the model Pluto 1.5 obtained after the inversion with the weighting factor $S = 1\,000\,\mathrm{ft\,s}$. The colour scale is the same as in Figure 5. The standard relative deviation of the velocity in the model from the full data grid is 3.261%, the "average Lyapunov exponent" of the model is $0.497\,\mathrm{s}^{-1}$.

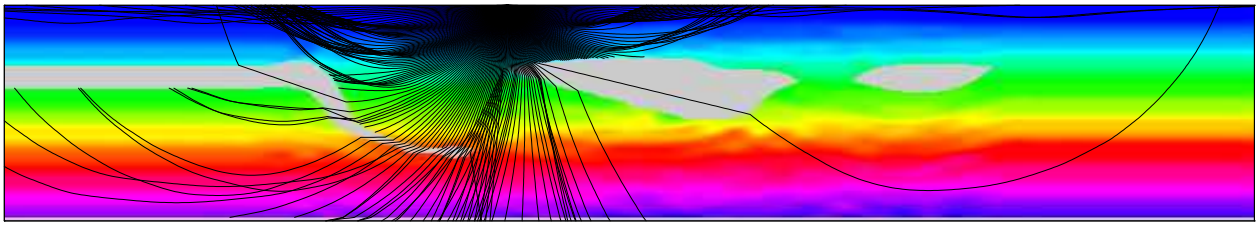

Figure 8: Rays computed by one–parametric shooting in the model Pluto 1.5 obtained after the inversion with $S = 125\,000\,\mathrm{ft\,s}$. The standard relative deviation of the velocity in the model from the full data grid is 2.611%, the "average Lyapunov exponent" of the model is $0.258\,\mathrm{s}^{-1}$.

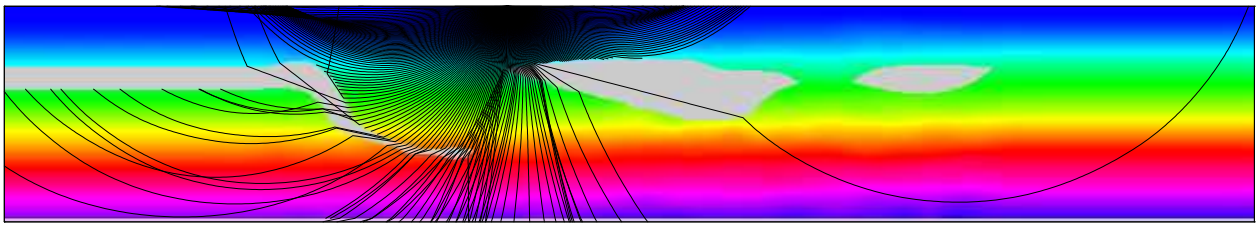

Figure 9: Rays computed by one–parametric shooting in the model Pluto 1.5 obtained after the inversion with $S = 1\,000\,000\,\mathrm{ft\,s}$. The standard relative deviation of the velocity in the model from the full data grid is 2.706%, the "average Lyapunov exponent" of the model is $0.075\,\mathrm{s}^{-1}$.

3.3 Smoothing the SEG/EAGE 3-D Salt Model for Kirchhoff migrations

The SEG/EAGE 3-D Salt Model (Aminzadeh *et al.* 1997) is specified in a form suitable for the GOCAD modelling software. Several interfaces in the model are stored in the form of triangulated surfaces, and the 3-D velocity cube is given. From the point of view of ray tracing, the gridded velocities and the points at the interfaces are not a model, because the values of the material parameters must be known at each point of the model volume for ray tracing. This example is thus principally different from the example of smoothing of the Hess model. On the other hand, the process of building of the Salt model is technically the same as the process of smoothing of the Hess model. Note that the generalization of the method from 2-D to 3-D is straightforward. The only problem is the limited memory of the computer being used, which disallows the use of all the data and of the denser parameterization of the model.

We construct two versions of a model for ray tracing: a smooth model without interfaces, and a model containing the salt body and some other selected interfaces. These interfaces are the ocean bottom, the interface limiting the salt body, the geopressure horizon, and the bottom flat interface.

The dimensions of the model are 13500 times 13500 times 4200 metres. The P-wave velocity is discretized on a grid of $676 \times 676 \times 210$ points with a spacing of $20 \times 20 \times 20\,\mathrm{m}$. This is a very large amount of data, and we immediately see

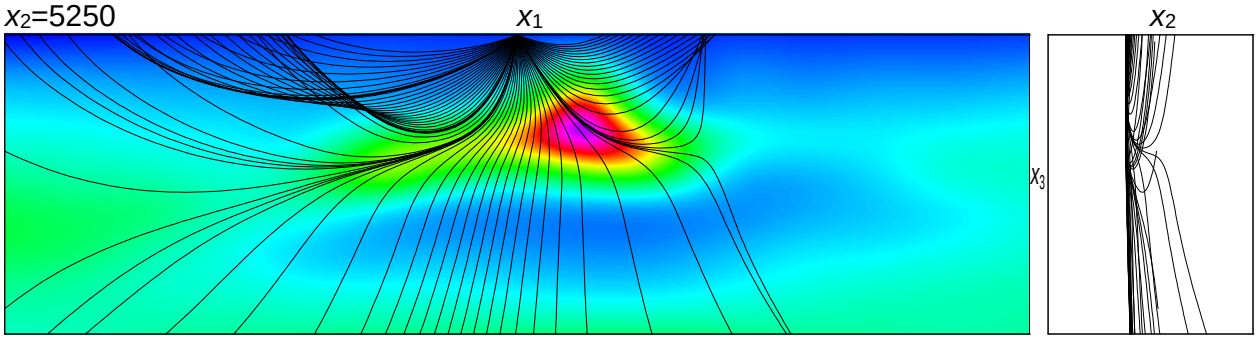

Figure 10: Rays computed by one–parametric shooting of a refracted wave in the x_1-x_3 plane in the smooth version of the Salt Model. The rays are projected onto the x_1-x_3 and onto the x_2-x_3 planes. The coordinates of the point source are [7000,5250,0] m. The x_1-x_3 plane is coloured according to the P-wave velocity in the x_1-x_3 section containing the point source. The colour scale ranges from dark blue for 1500 $\mathrm{m\,s^{-1}}$ in the water to red for 4450 $\mathrm{m\,s^{-1}}$ in the salt body. The horizontal extents of both the x_1-x_3 and x_2-x_3 sections are 14000m, the vertical extents of the sections are 4200m. The reader is reminded that the standard relative deviation of the velocity in the model from the data is 8.22%.

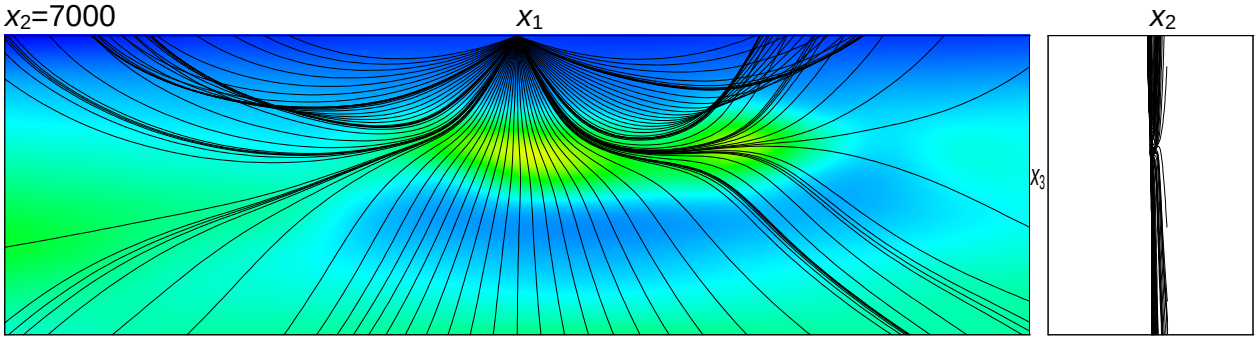

Figure 11: Rays computed by one–parametric shooting of a refracted wave in the x_1-x_3 plane in the smooth version of the Salt Model. The x_2 coordinate of the point source and of the velocity section is now 7000 m. The colour scale is the same as in Figure 10.

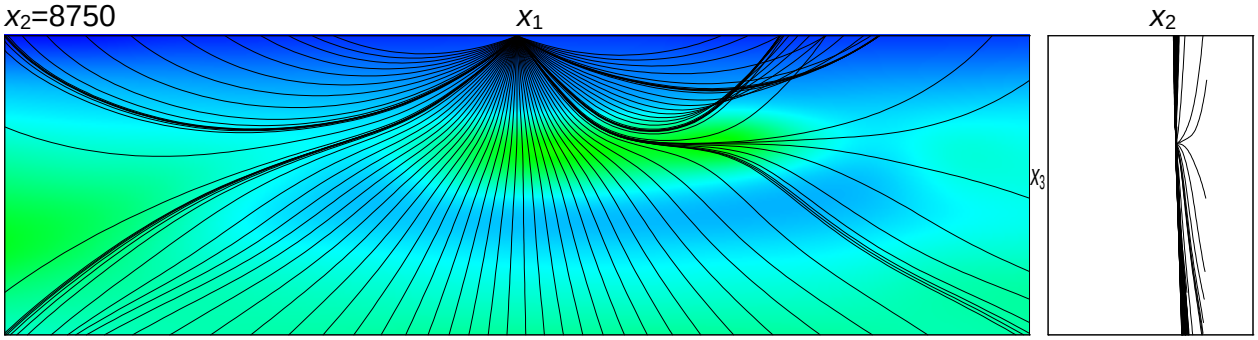

Figure 12: Rays computed by one–parametric shooting of a refracted wave in the x_1-x_3 plane in the smooth version of the Salt Model. The x_2 coordinate of the point source and of the velocity section is 8750 m. The colour scale is the same as in Figure 10.

that a much sparser grid must be used for the data for the inversion, similarly as in the case of model Pluto 1.5. For all the interfaces, except the salt interface, we may use the triangulated surfaces in the GOCAD representation as the data for inversion. In case of the salt interface, the corresponding GOCAD file contains all the triangles of the interface. We tried to model the interface by a single surface, but all our attempts failed, and the salt interface must be fitted by at least two surfaces. We thus generate two files according to the discontinuity in the velocity cube corresponding to the surface of the salt body: one file with the points at the top of the salt, and the other with the points at the bottom of the salt.

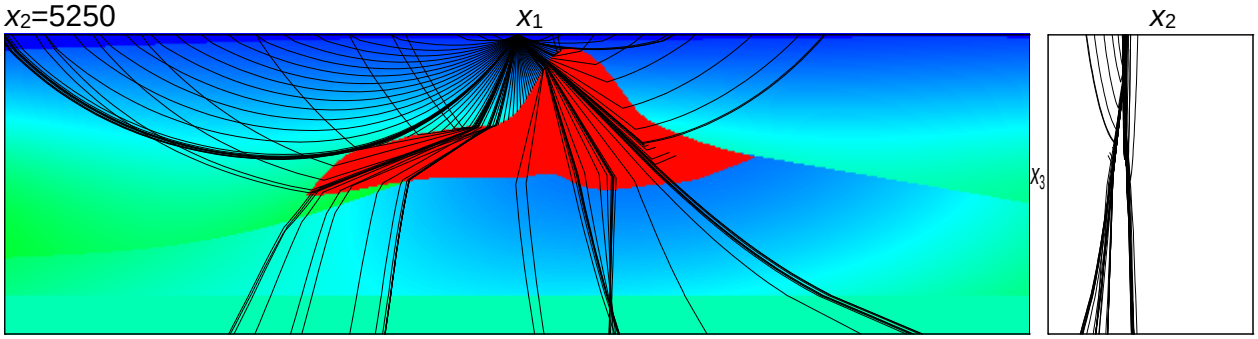

Figure 13: Rays computed by one–parametric shooting of a refracted wave in the $x_1 - x_3$ plane in the Salt Model, the version with interfaces. The x_2 coordinate of the point source and of the velocity section is 5250 m. The colour scale is the same as in Figure 10. The reader is reminded that the standard relative deviation of the velocity in the model from the data is 5.24%.

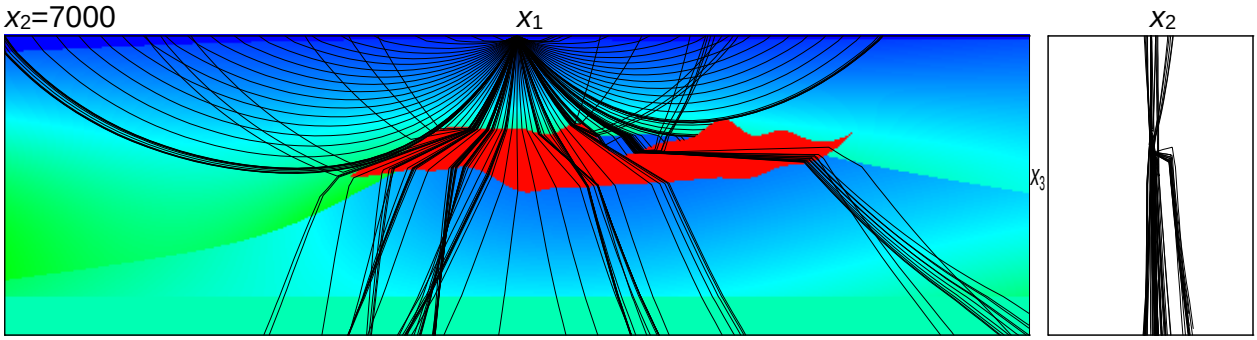

Figure 14: Rays computed by one–parametric shooting of a refracted wave in the $x_1 - x_3$ plane in the Salt Model, the version with interfaces. The x_2 coordinate of the point source and of the velocity section is 7000 m. The colour scale is the same as in Figure 10.

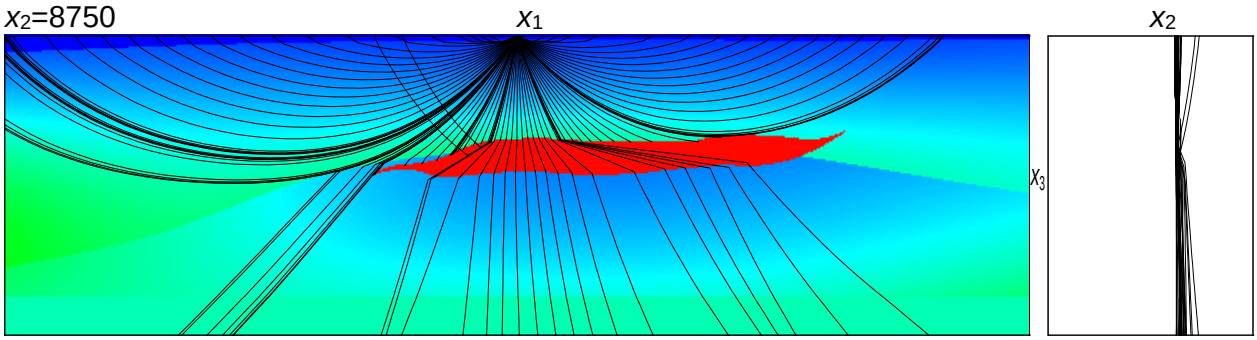

Figure 15: Rays computed by one–parametric shooting of a refracted wave in the $x_1 - x_3$ plane in the Salt Model, the version with interfaces. The x_2 coordinate of the point source and of the velocity section is 8750 m. The colour scale is the same as in Figure 10.

The best obtained model without interfaces, which satisfies our requirements with respect to the Lyapunov exponent, has the standard relative deviation of the velocity in the model from the original data cube 8.22% (Figures 10, 11, 12). The best obtained model with the selected interfaces has the standard relative velocity deviation 5.24% (Figures 13, 14, 15). For more detailed description of the process of inversion refer to Bulant (2001).

We performed several tests of ray tracing in the models obtained after the inversions. As it is difficult to clearly display the results of 3-D ray tracing, we decided to shoot the rays only in the direction of the $x_1 - x_3$ plane (one–parametric shooting in a 3-D model). We then projected the computed rays onto the x_1–x_3 plane and onto the x_2–x_3 plane. The projected rays together with the velocity sections corresponding to the x_2 coordinates of the sources are displayed in Figures 10 to 15.

Sobolev norms in model building

Conclusions

The minimization of the Sobolev norm of the model during linearized inversion enables us to control the model parameters unresolved by the data being fitted, while the parameters determined by the data remain almost unchanged. It enables us to minimize not only the difference between the data and the model, but, for many computational methods, also the difference between the exact solution and the results obtained by the considered approximate numerical method to be used for calculating wavefields in the model.

The smoothness of the velocity field of the models constructed for the ray methods may be quantitatively described in terms of the "average Lyapunov exponent" for the model. The "average Lyapunov exponent" may be approximated by the square root of the corresponding Sobolev norm of the model. This enables us to determine the quantitative criteria on the models, so as to be suitable for ray tracing, in terms of Sobolev scalar products. The criteria then allow us to construct the optimum models of geological structures for ray tracing, either by smoothing given rough models, or by inversion of seismic data.

The numerical examples demonstrate the application of Sobolev norm to the regularization of the ill–conditioned inversion. The behaviour of the model functions in the regions not illuminated by the data is controlled by the Sobolev norm.

The example of smoothing model Hess shows, how the smoothing of the velocity field by including the Sobolev norm in the velocity inversion regularizes the chaotic behaviour of rays, while the velocity field changes only slightly with the standard relative deviation of 1.8 per mille. Note that the standard relative velocity deviation is equivalent to the standard relative travel–time deviation for very short rays.

The example of building the SEG/EAGE Salt Model demonstrates the use of Sobolev norms in inverting 3-D data.

References

Aminzadeh, F., Brac, J., Kunz, T. (1997): 3-D Salt and Overthrust Models. SEG/EAGE 3-D Modeling Series No.1., Soc. Explor. Geophysicists, Tulsa.

Bulant, P. (2001): Sobolev scalar products in the construction of velocity models — application to model Hess, to SEG/EAGE Salt Model, and to model Pluto 1.5. In: Seismic Waves in Complex 3-D Structures, Report 11, pp. 133–159, Dep. Geophys., Charles Univ., Prague.*

Bulant, P. (2002): Sobolev scalar products in the construction of velocity models: Application to model Hess and to SEG/EAGE Salt Model. Pure and appl. Geophys., **159**, 1487–1506.*

Klimeš, L.: (2000): Sobolev scalar products in the construction of velocity models. In: Seismic Waves in Complex 3-D Structures, Report 10, pp. 15–40, Dep. Geophys., Charles Univ., Prague.*

Klimeš, L. (2002a): Lyapunov exponents for 2-D ray tracing without interfaces. Pure and appl. Geophys., **159**, 1465–1485.*

Klimeš, L. (2002b): Application of the medium covariance functions to travel–time tomography. Pure and appl. Geophys., **159**, 1791–1810.*

Tarantola, A. (1987): Inverse Problem Theory. Elsevier, Amsterdam.

Žáček, K. (2002): Smoothing the Marmousi model. Pure and appl. Geophys., **159**, 1507–1526.*

Acknowledgments

This research has been supported by the Grant Agency of the Czech Republic under Contracts 205/01/0927 and 205/01/D097, by the Grant Agency of the Charles University under Contract 237/2001/B-GEO/MFF, by the Ministry of Education of the Czech Republic within Research Project J13/98 113200004, and by the members of the consortium "Seismic Waves in Complex 3-D Structures" (see http://sw3d.mff.cuni.cz).

---

*Available online at http://sw3d.mff.cuni.cz.